Constraint Current Control for Grid-Connected Power Inverter

[1]**Masud Ibrahim,**
[2]**Safiyanu Muhammad Babale,** [3]**Ammar Muhammad Ibrahim &** [4]**Sulaiman Hassan**

[1,2,3&4]*Department of Electrical Engineering, School of Technology, Binyaminu Usman Polytechnic Hadejia, Jigawa State*

Keywords:
Grid-connected
Inverter, LQR,
Constraint handling,
Optimization

Corresponding Author:
Masud Ibrahim

Abstract

Recent study has paid much attention in the areas of renewable energy (solar and wind) as an alternative method to derive electrical power rather than going by fossil fuels (coal, natural gases etc.) which constantly emits carbon dioxide and other harmful substances into the atmosphere. The emission of these undesirable harmful substances into the atmosphere have caused climatic changes for example global warming, acid rain, low precipitations and unwanted desert encroachment. These badly affect the quality life of humans and animals. In response to these problems, methods of reducing carbon content emissions become necessary through the use of renewable energy sources (Photovoltaic system, Wind power, Fuel cell etc.). As a result, research on grid-connected inverter have recently become a very hot topic as a means of interfacing renewable energy sources to utility grid. With good interfacing, the renewable energy sources can be able to solve not only the problem of carbon emissions into the atmosphere but also to efficiently support the grid from increased demand of electrical power. Thus, this research has focused on designing a constraint current controller for grid-connected inverter using linear quadratic regulations (LQR) method. The idea of using LQR control design as opposed to classical PI controller is that The LQR provides optimal current control by careful tuning of the input and state weighting matrices and therefore systematic control design can be achieved. Another advantage of LQR method is that constraint handling can be address through an offline optimization technique. This is necessary in order to protect the inverter system components (semiconductor switches) and improve its reliability.

Background to the Study

Inverter converts DC to AC voltage through semiconductor devices (IGBTs, Thyristors, and MOSFETs etc.). Grid-connected inverter is required to deliver power to the grid in order to support loads. Grid connected inverter is widely used nowadays to integrate many renewable energy sources such as PV, Wind, Fuel cell etc. The essence of using renewable energy sources is to mitigate the amount of carbon emission into the atmosphere, which can result in undesirable climatic change. Several methods of current control for grid connected inverter system have been investigated for many years. The current control for grid-connected inverter is useful to send active and reactive power to the utility grid. Also, power factor correction and active filtering is possible with current control to improve the grid power quality. One of the techniques employed for current control is classical PI controller, which is used for tracking of constant (DC) reference current signal. This type of control only works in synchronous reference frame (DQ) and require decoupling to achieve effective control [2][13]. In stationary reference frame (Alpha-Beta), PI controller led to large steady state error as it cannot track AC reference current signal. Hence, classical PI controller has perfect tracking at only zero frequency (DC). In order to track an AC reference current with zero steady state error, the so called Proportional resonant (PR) controller should be used [3][10][14][15][19]. However, the PR controller tracks a given reference current at specific frequency called resonant frequency. Any slight deviation of resonant frequency will lead to poor performance tracking. Therefore, for a grid where frequency fluctuates, a PLL should be implemented to synchronize the phase angle as well as the frequency of the grid by correcting any deviation between the grid and inverter [1][17][18]. A linear quadratic regulation (LQR) is an optimal control method that solve an optimization problem to minimize a given cost function. Minimization of cost function can be achieved by careful tuning of input and state weighting matrices (Q and R) [4][5][6][9]. LQR is in effect a proportional controller and thus does not provide reference tracking with zero steady state error. To achieve current control with zero steady state error, the state variable error should be formulated in the cost function [8][12][16]. For a constant reference tracking, an integral control is augmented in the LQR design (PI controller) to eliminate the steady state error. For AC reference tracking, a resonant controller is augmented in the LQR design (PR controller) to eliminate AC steady state errors [20][21][22]. Constraints design is necessary for the protection of inverter system. For example, the rated semiconductor voltage and current, DC-link rated voltage, power losses limitation, overshoot, non-minimum phase behavior etc. [14]. Therefore, an offline closed loop predictions using state space model of VSI can be applied to check whether the constraints design being imposed in the control are satisfied or not [7][11].

In general, this research investigates an LQR design method for the development of constraint current controller for grid connected power inverter. The idea behind using LQR is that it solves an optimization problem and deliver an optimal control. Through this optimization, it allows a constraint to be imposed in the control design and compute a feasible solution. As a result, the inverter switching components can be protected and thus improve the reliability and efficiency of the overall system. The LQR design method

is investigated in both DQ frame and Alpha-beta frame. In DQ frame, the LQR is design to control a DC current signal and thus PI controller is used. However, in Alpha-beta frame, the LQR is design to control AC current signals and thus PR controller is used.

Methodology

A typical three-phase voltage source inverter VSI configuration is presented in fig1.The output voltage or current of the inverter is controlled by applying appropriate pulse signals to six IGBTs switches (S1 to S6). These switches convert the DC into AC output signal, which eventually connected to the grid. For grid connected inverter, the objective is to control the active and reactive power, and this depend on the current supplied into the grid.it is therefore imperative to derive the mathematical model of the inverter circuit which allow the control of the current. The mathematical modelling of VSI can be realized either with direct-quadrature (DQ) or in Alpha-Beta (αβ) transformations [Kom+16]. With these transformations, the state space model of VSI can be obtained.
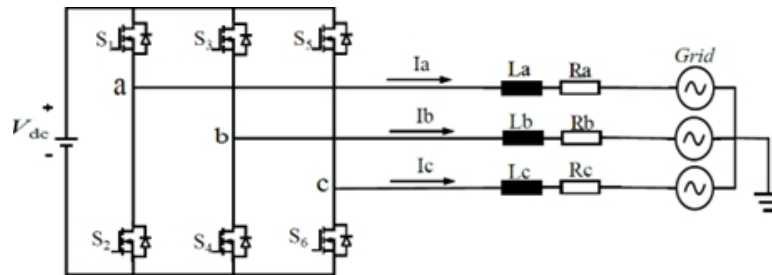

Fig. 1: Schematic diagram of grid-connected inverter

Modelling of the Inverter

Before applying any control scheme, it is necessary to understand the behavior of the system (plant). In this case, the inverter configuration has to be modelled. The modelling is done by obtaining the differential equation (DE) from the single-phase equivalent circuit shown in fig 2. The DE of the single inverter is presented in Eqn. (1).
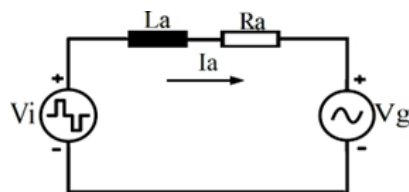

Fig. 2: Single-phase equivalent circuit

$$\frac{di_a}{dt} = -\frac{R_a}{L_a}i_a + \frac{1}{L_a}V_i - \frac{1}{L_a}V_g \qquad (1)$$

Where: i, is the output voltage of the inverter, Vag is the grid voltage acting as disturbance, and Ra, La are impedance for the single-phase equivalent circuit of VSI.

For balanced three phase system, the impedance are equal. Thus, (Ra =Rb = Rc = R) and (La = Lb = Lc = L). Then the DE of the three phase circuit is formulated in a compact form as:

$$\frac{di_{abc}}{dt} = -\frac{R}{L}i_{abc} + \frac{1}{L}V_{abci} - \frac{1}{L}V_{abcg} \qquad (2)$$

State space modelling with Alpha-Beta (αβ) frame
VSI inverter can be modelled in Alpha-Beta frame (stationary reference frame) with the aid of Clarke transformation. Clarke transformation converts three phase voltages or currents into orthogonal αβ0 components as depicted in Eqn. (3). The αβ0 components are time varying quantities (AC) shifted by 90 degrees and both have the same peak value as the three phase voltages/currents as shown in Fig3. The α-component is responsible for active power control while the β-component is responsible for reactive power control. It is also important to highlight that if three phase system voltages or currents are balanced, then the third components '0' is neglected and thus reduce to two components αβ.

$$\begin{bmatrix} v_\alpha \\ v_\beta \\ v_0 \end{bmatrix} = \begin{bmatrix} 1 & -\frac{1}{2} & -\frac{1}{2} \\ 0 & \frac{\sqrt{3}}{2} & -\frac{\sqrt{3}}{2} \\ \frac{1}{\sqrt{2}} & \frac{1}{\sqrt{2}} & \frac{1}{\sqrt{2}} \end{bmatrix} \begin{bmatrix} v_a \\ v_b \\ v_c \end{bmatrix} \qquad (3)$$

By applying Clarke transformation in Eqn. (2), the DE of the αβ frame can be obtained as presented in Eqn. (4).

$$\frac{di_{\alpha\beta}}{dt} = -\frac{R}{L}i_{\alpha\beta} + \frac{1}{L}V_{\alpha\beta i} - \frac{1}{L}V_{\alpha\beta g} \qquad (4)$$

The standard state space LTI system in continuous form is depicted in Eqn. (5and 6)

$$\dot{x}(t) = Ax(t) + Bu(t) + Ew(t) \qquad (5)$$
$$y(t) = Cx(t) + Du(t) \qquad (6)$$

By comparing Eqn 4, 5 and 6, the state space variables can be obtained with $x = \begin{bmatrix} i_\alpha \\ i_\beta \end{bmatrix}$, u= $\begin{bmatrix} V_{\alpha i} \\ V_{\beta i} \end{bmatrix}$, w= $\begin{bmatrix} V_{\alpha g} \\ V_{\beta g} \end{bmatrix}$ are state variables, inputs and disturbance respectively. The state space parameters are given as follows:

$$A = \begin{bmatrix} -\frac{R}{L} & 0 \\ 0 & -\frac{R}{L} \end{bmatrix}, B = \begin{bmatrix} \frac{1}{L} & 0 \\ 0 & \frac{1}{L} \end{bmatrix}, E = \begin{bmatrix} -\frac{1}{L} & 0 \\ 0 & -\frac{1}{L} \end{bmatrix}, C = \begin{bmatrix} 1 & 0 \\ 0 & 1 \end{bmatrix}, D=0.$$

State space modelling with DQ frame
The modelling of VSI in DQ frame (synchronous reference frame) is done with the aid of Park transformation. Park Transformation converts three-phase system into dq0. The three phase voltages or currents are first transformed into orthogonal (αβ0) components.

Then the resulting αβ0 components is then rotated about a fixed angle θ to form the dq0 which are DC quantities. θ is a function of grid frequency (w) obtained with phase locked loop that locks the original three phase voltages and align them with dq axis. For a balanced three phase system, the d-component is constant (DC) with the same peak value as the original three phase voltages/currents while the q-components is zero and the '0' components is often neglected. The d-component is used to control the active power while the q-component for reactive power. The DQ transformation is given in Eqn. (7).

$$\begin{bmatrix} v_d \\ v_q \\ v_0 \end{bmatrix} = \begin{bmatrix} \cos\theta & \sin\theta & 0 \\ -\sin\theta & \cos\theta & 0 \\ 0 & 0 & 1 \end{bmatrix} \begin{bmatrix} v_\alpha \\ v_\beta \\ v_0 \end{bmatrix} \qquad (7)$$

By applying Park transformation in Eqn. (2), the DE of the DQ frame is obtained as depicted in Eqn. (8).

$$\frac{di_{dq}}{dt} = -\frac{R}{L}i_{dq} + \frac{1}{L}V_{dqi} - \frac{1}{L}V_{dqg} - \omega\begin{bmatrix} 0 & -1 \\ 1 & 0 \end{bmatrix} \qquad (8)$$

With $x = \begin{bmatrix} i_d \\ i_q \end{bmatrix}$, $u = \begin{bmatrix} V_{di} \\ V_{qi} \end{bmatrix}$, $w = \begin{bmatrix} V_{dg} \\ V_{qg} \end{bmatrix}$ are state variables, inputs and disturbances respectively. The ω represent the grid frequency.

The state space parameters of the DQ frame is extracted as follows;

$$A = \begin{bmatrix} -\frac{R}{L} & \omega \\ -\omega & -\frac{R}{L} \end{bmatrix}, B = \begin{bmatrix} \frac{1}{L} & 0 \\ 0 & \frac{1}{L} \end{bmatrix}, E = \begin{bmatrix} -\frac{1}{L} & 0 \\ 0 & -\frac{1}{L} \end{bmatrix}, C = \begin{bmatrix} 1 & 0 \\ 0 & 1 \end{bmatrix}, D = 0.$$

Once the state space model of VSI is obtained, the LQR method can be designed to control the current variables in both DQ and αβ frame.

Linear Quadratic Regulation (LQR)
Linear Quadratic regulation (LQR) is a proportional (P-type) controller with gain Ks to regulate all state variables to the origin. However, the interest here is to control the current variables to a desired reference value. Hence, a reference tracking is introduced in the LQR. An LQR is a method of designing an optimal feedback gain by systematic tuning/tradeoff between the importance of performance and control effort, which are formulated in the cost function. The cost function represents the measure of the quality of the closed loop behavior which comprises of settling time, maximum overshoot, rise time, offset, peak input value etc. Large cost function implies poor system performance while small cost function implies good performance. The cost function and control law in continuous form is depicted in Eqn. (9) and Eqn. (10) respectively.

$$\text{Min}\, u, x \qquad J = \frac{1}{2}\int_0^\infty (x^T(t)Qx(t) + u^T(t)Ru(t))dt \qquad (9)$$
$$u(t) = -K_s x(t) \qquad (10)$$

where: Q ≥ 0 is a diagonal state weighting matrix which penalizes the state deviation and thus the control error, R > 0 is a diagonal input weighting matrix which penalizes the input deviation and thus the control effort, u is the control law and x is the state variable.

By careful choice of the state weighting matrix Q and input weight matrix R [5], then an optimal feedback gain Ks is determined by solving the cost function which gives the minimum value. The Ks value is computed using the relation in Eqn. (11) and depends on P which is obtained by solving algebraic Riccati equation (ARE) presented in Eqn (12). The ARE is solvable if there exist a semi definite matrix P ≥ 0.Once the optimal feedback gains is obtained, the closed loop system stability is guaranteed.

$$K_s = R^{-1}B^T P \qquad (11)$$
$$PA + A^T - PBR^{-1}B^T P + Q = 0 \qquad (12)$$

Linear quadratic regulation in DQ-frame
In DQ frame the control variables are i_d and i_q. The LQR should be designed to control these variables to their respective reference value. Therefore, the control law is modified to include a pre-filter gain K_f responsible for reference tracking. Nevertheless, the pre-filter is not enough to provide good reference tracking as it doesn't provide robustness with respect to parameter uncertainties (A, B,C),disturbances and measurement noises. Thus, steady state error is always present. In order to provide good robustness against these uncertainties, the integral control is introduced in the control law. Therefore, additional integral state formulated in Eqn. (13,14) is augmented with the original state space of Eqn. (5,6). The idea behind this is to integrate the error between the measured output current and the reference current until it becomes zero. The combined integral action is depicted in Eqn. (15) and the overall control input is expressed in Eqn. (16).

$$\dot{x}_i(t) = r(t) - y(t) \qquad (13)$$
$$\dot{x}_i(t) = r(t) - Cx(t) \qquad (14)$$
$$\begin{bmatrix} \dot{x}(t) \\ \dot{x}_i(t) \end{bmatrix} = \begin{bmatrix} A & 0 \\ -C & 0 \end{bmatrix} \begin{bmatrix} x(t) \\ x_i(t) \end{bmatrix} + \begin{bmatrix} B \\ 0 \end{bmatrix} u(t) + \begin{bmatrix} 0 \\ 1 \end{bmatrix} r(t) \qquad (15)$$
$$u(t) = -K_s x(t) - K_i x_i(t) + K_f r(t) \qquad (16)$$

Since the new state space is formed in Eqn. (15), therefore new parameters are also formed as follows:

$$A_{aug} = \begin{bmatrix} A & 0 \\ -C & 0 \end{bmatrix}, B_{aug} = \begin{bmatrix} B \\ 0 \end{bmatrix}$$

The new input matrix R_{aug} and state-weighting matrix Q_{aug} is formed with corresponding dimension of A_{aug} and B_{aug}. The augmented state feedback gains K_{aug} can determined using the same formula as in Eqn. (11). Once K_{aug} is computed, the state feedback gains K_s and Integral gains K_i can be extracted. The pre-filter gain K_f of the augmented system is obtained from the relation presented in Eqn. (17).

$$K_f = (-C(A - BK_s)^{-1}B)^{-1} \qquad (17)$$

The LQR current control for the DQ frame is summarized with a block diagram shown in Fig3.
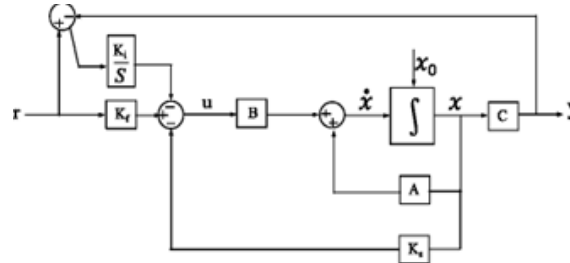

Fig. 3: LQR current controller with integral action (DQ-frame)

Linear Quadratic Regulation in αβ-Frame

It should be recalled that Alpha-Beta transformation convert three phases into orthogonal αβ components which are time varying quantities (AC signal). Therefore, the control variables are i_α and i_β. The control aim in αβ is to track an AC reference signal as opposed to constant DC reference signal as in DQ-frame. To design a current control to track a given reference AC signal, a resonant controller should be used. A resonant controller operates just like the integral action in DQ-frame and is capable of tracking an AC signal with zero steady state error at a specified frequency called resonant frequency. For perfect tracking of reference current (zero steady state error), it is required at resonant frequency, the magnitude of the closed loop should be one (1) and the phase shift should be zero (0). One major drawback with resonant controller is that it is very sensitive to frequency variations. Slight change in frequency can lead to large steady state error (poor tracking). This problem can be solved with the aid of phase locked loop (PLL). The resonant controller transfer function is formulated in Eqn. (18).

$$G_{RC}(s) = \frac{K_c S}{s^2 + n^2 \omega^2} \qquad (18)$$

From transfer function in Eqn. (18), the tuning parameter is K_c which determines the amplitude gain at resonant frequency. To obtain this parameter using LQR method, a resonant state space should be augmented in the plant model in similar fashion as done in DQ-frame with integral action. The state space of resonant controller for αβ is depicted in Eqn. (19).

$$\dot{x}_c(t) = A_c x_c(t) + B_c e(t) \qquad (19)$$
$$y_c(t) = C_c x_c(t) \qquad (20)$$
$$e(t) = r(t) - Cx(t) \qquad (21)$$

The augmented state space is expressed as:

$$\begin{bmatrix} \dot{x}(t) \\ \dot{x}_c(t) \end{bmatrix} = \begin{bmatrix} A & 0 \\ -B_c C & A_c \end{bmatrix} \begin{bmatrix} x(t) \\ x_c(t) \end{bmatrix} + \begin{bmatrix} B \\ 0 \end{bmatrix} u(t) + \begin{bmatrix} 0 \\ B_c \end{bmatrix} + r(t) \qquad (22)$$

With $A_{aug} = \begin{bmatrix} A & 0 \\ -B_c C & A_c \end{bmatrix}$, $B_{aug} = \begin{bmatrix} B \\ 0 \end{bmatrix}$

Similarly, the augmented feedback matrix K_{aug} is found from Eqn. (11). The gain matrix K_s and K_c can be extracted from K_{aug}. The resonant current controller block diagram for αβ-frame is shown in fig. 4. The overall control law is formulated in Eqn. (23).
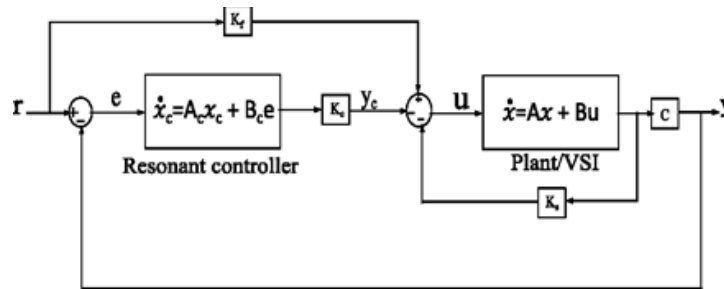
$$u(t) = -K_s x(t) - K_c x_c(t) + K_f r(t) \quad (23)$$

Fig. 4: Resonant current controller (αβ -frame)

Optimization and Constraint handling
Constraint designs are necessary for components protection to improve reliability and safety. For instance, semiconductor rated voltage and current, DC-link rated voltage and filter saturation. Constraints are classified into hard and soft constraints. Example of soft constraints are output constraints, maximum overshoot, settling time etc. Hard constraints include input constraint, non-minimum phase behavior etc. To handle constraints, an algorithm is developed with a closed loop prediction. The predictions is done in an offline mode using discrete state space model. Still online predictions is possible but tedious and is still under research (for example MPC) [7][11]. The algorithm checks whether these constraints are satisfied or not. This is sort of user verification to check for constraints satisfaction. The procedures for the constraints design are summarized in the flow chart shown in fig 5.
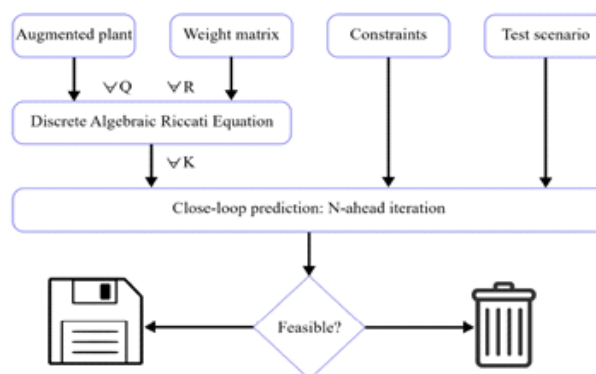

Fig 5: Flow chart for constraint verification

The pool of parameters Q and R are chosen to compute the corresponding optimal gains K. the values of these gains are used for simulation to observe whether the constraints are

met or not. If the Q and R gives values of K that does not respect the constraints, then the solution is not feasible. Hence the values of Q and R should be changed to get new values of K until a feasible solution is obtained which doesn't violate the constraints.

Simulation Results and Discussions
The control design and simulations are done with the aid of Matlab and PLECS software. The Inverter specifications and power ratings used are given in Table1.The current control simulations are done in both DQ-frame and αβ frame. The constraints imposed for the controller are provided in Table2. The maximum output current is chosen to be 10A for each phase, which reflect the standard rating for household outlet [1]. The constraint of this output is design to be less than the maximum overshoot of 20 percent i.e. 12A. Other constraints which should be respected are settling time define to be less than the time constant and the output current should not have zeros on the right half plane (RHP).

Table 1: Inverter specifications

Parameters	Specifications
V_{dc}	700V
V_{rms}	230V
f_g	50Hz
f_{sw}	10KHz
f_s	10KHz
L	2mH
R	10mΩ

Table 2: Constraints specifications

Constraints	Limits
Rate Input voltage (Δu)	$0 < \Delta u \leq 25V$
Output current (i)	$0 < i \leq 12A$

The tuning values of the weighting matrices Q and R is not straight forward as to which value should be used. Nonetheless, as a benchmark the state weighing matrix can be choosing as the inverse of the maximum of the between the square of the states. This is also treated the same for the input weighting matrix. Furthermore, other tuning methods can be found in literatures [5]. For this simulation, the pool Q and R were chosen between $1e^{-6}$ to $1e^{6}$ and are values are changed by multiple of 10. This means that a possible of 144 different combinations of Q and R were used. Similarly, 144 optimal gains K were also computed. With these pools of gains being computed, the control law is set. The constraint design is checked with closed predictions over a prediction horizons N until a feasible solution is obtained. The prediction horizon is selected to have a prediction with t=1s.Thus with the sampling period of $T_s = \frac{1}{f_s}$ which is equals to $10^{-4}s$, number prediction horizons can be computed as follows:

$$N = \frac{t}{T_s} = \frac{1}{10^{-4}} = 10000 \ horizons \qquad (24)$$

The simulations result for input voltages u_d and u_q, output currents I_d and I_q and error for DQ-frame current control are illustrated in fig6 and fig7 respectively. It could be observed that, there is a step change in the reference current at 0.2s and the output current instantly track the reference current with an overshoot. It could be justified that the constraint design with a maximum overshoot of 12A is still respected. Furthermore, from the input plot, it can be seen that with these step change, the input constraint of 25V is not violated. To see the effect of a switched model and the averaged (simulated) model, the comparison between the three-phase switched current of the inverter and that of the simulated plot is provided in fig. 8 and fig. 9 respectively. The control input and the output error for switched model in DQ frame are presented in fig. 10 and fig. 11 respectively.
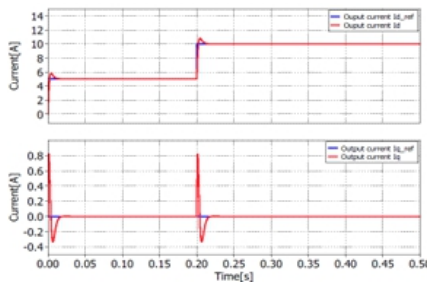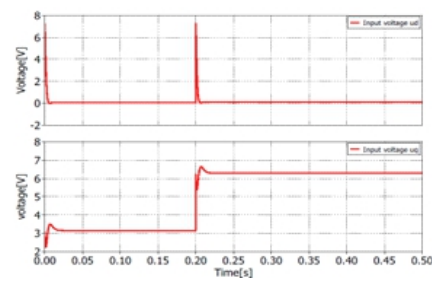

Fig 6: Averaged output currents I_d and I_q (DQ)
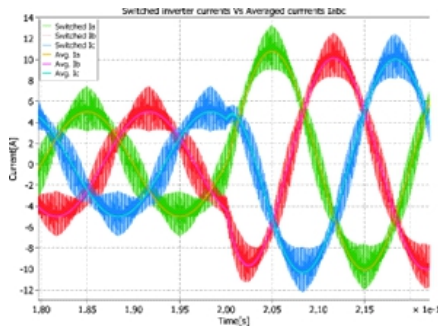

Fig 7: Averaged control inputs u_d and u_q (DQ)

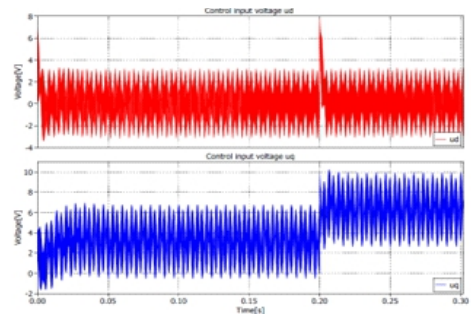**Fig 8:** Switched output currents I_a, I_b and I_c (DQ)

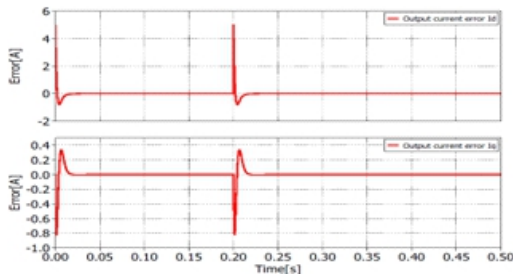**Fig 9:** Switched control inputs u_d, and u_q (DQ)
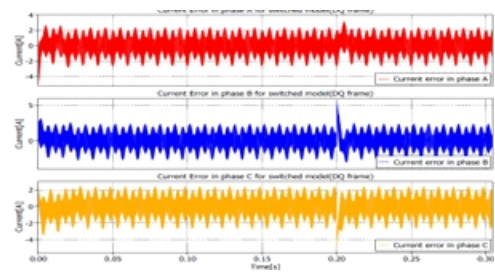
Fig 10: Averaged current errors (DQ)

Fig 11: Switched current errors (DQ)

Similarly, the same simulations results are provide for Alpha-Beta frame. The input voltages u_α and u_β, output currents i_α and i_β and error for αβ frame current control are illustrated in fig.12 and fig.13 respectively. Just like in the DQ-control, it could be seen as well in αβ frame that the output currents and the input voltages do not violate their constraints. However, there is one observation with the plot of three phase currents between switched model and averaged model as presented in fig14 and fig15.It could be carefully seen that there are more switching ripples present in DQ-frame compared to αβ frame. Furthermore, for the same target value of the output currents, the control effort required for αβ frame is slightly lower than that of the DQ-frame. The control input and the output error for switched model in αβ frame are presented in fig.16 and fig.17 respectively.
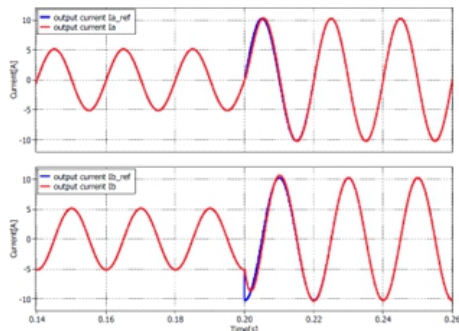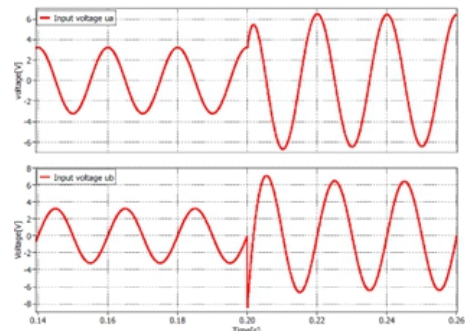

Fig12. Averaged output currents i_α and i_β (αβ)

Fig13. Averaged control inputs u_α and u_β (αβ)
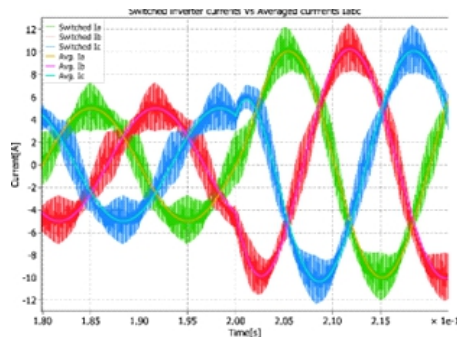
Fig14. Switched output currents i_α and i_β (αβ)
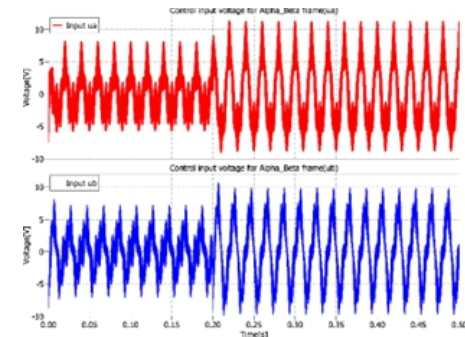

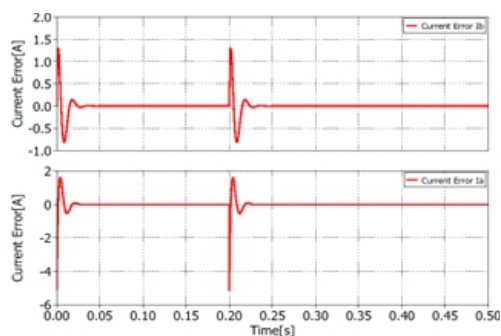**Fig15.** Switched control inputs u_α and u_β (αβ)

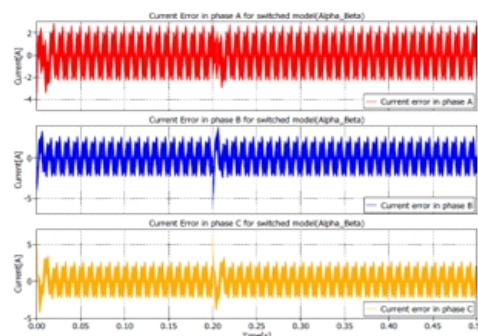**Fig 16.** Averaged current errors ($\alpha\beta$)

Fig 17. Switched Current errors ($\alpha\beta$)

Conclusions

In this research, an LQR controller is design to control the currents of the VSI. The VSI is first modelled before the control scheme is applied. The control is applied to two different scenarios. The first scenario is the DQ frame where three phase is transform into constant dq variables using park transformation. This scenario requires a constant reference tracking and is achieved using LQR controller with integral control. The second scenario is the $\alpha\beta$ frame in which the three phase is transform into time varying $\alpha\beta$ variables. Thus, this scenario requires an AC reference tracking and is achieved using resonant controller.

The constraints is important in the controller design for the safety and reliability of the inverter system components. Consequently, an offline closed loop predictions is used to check the feasible solution that respect the constraint being imposed in the control design.

Simulations results were obtained with the aid of Matlab and PLECS software. The performance of constraints current controller for both DQ and $\alpha\beta$ frame were shown in the research. It was observed that in DQ frame, it requires more control effort and computational burden, which result from the transformation. Furthermore, there is more ripples in DQ frame compared to $\alpha\beta$ frame. On the other hand, in $\alpha\beta$ frame, the control is very sensitive with frequency variations. This means that its large errors could be realized from slight frequency variation in the grid and eventually could lead to poor performance.

Reference

[1] Afshari, E., Moradi, G. R., Yang, Y., Farhangi, B., & Farhangi, S. (2017). A review on current reference calculation of three-phase grid-connected PV converters under grid faults, *2017 IEEE Power and Energy Conference at Illinois (PECI)*, 1–7. https://doi.org/10.1109/PECI.2017.7935761

[2] Bacha, S., Munteanu, I., & Bratcu, A. I. (2014). *Power electronic converters modeling and control*, Springer London. https://doi.org/10.1007/978-1-4471-5478-5

[3] Hackl, C. M. (2016). *On the equivalence of proportional-integral and proportional-resonant controllers with anti-windup* (arXiv:1610.07133). arXiv. http://arxiv.org/abs/1610.07133

[4] Harnefors, L., Yepes, A. G., Vidal, A., & Doval-Gandoy, J. (2014). Passivity-based stabilization of resonant current controllers with consideration of time delay. *IEEE Transactions on Power Electronics*, *29*(12), 6260–6263. https://doi.org/10.1109/TPEL.2014.2328669

[5] Hasanzadeh, A., Edrington, C. S., & Mokhtari, H. (2011). A novel LQR based optimal tuning method for IMP-based linear controllers of power electronics/power systems. *IEEE Conference on Decision and Control and European Control Conference*, 7711–7716. https://doi.org/10.1109/CDC.2011.6160726

[6] Holliday, D., Williams, B. W., Ben-Brahim, L., Massoud, A., & Azani, H. (2014). Multiloop control strategy for grid-interfaced Three-phase voltage source inverter with passively damped LLCL-filter. *3rd Renewable Power Generation Conference (RPG 2014)*, 8.44-8.44. https://doi.org/10.1049/cp.2014.0929

[7] Judewicz, M. G., Gonzalez, S. A., Echeverria, N. I., Fischer, J. R., & Carrica, D. O. (2016). Generalized predictive current control (GPCC) for grid-tie three-phase inverters, *IEEE Transactions on Industrial Electronics*, *63*(7), 4475–4484. https://doi.org/10.1109/TIE.2015.2508934

[8] Kuperman, A. (2015). Proportional-Resonant current controllers design based on desired transient performance, *IEEE Transactions on Power Electronics*, *30*(10), 5341–5345. https://doi.org/10.1109/TPEL.2015.2408053

[9] Li, Y., Zhang, J., Hao, Z., & Tian, P. (2021). Improved PR control strategy for an LCL three-phase grid-connected inverter based on active damping. *Applied Sciences*, *11*(7), 3170. https://doi.org/10.3390/app11073170

[10] Manoloiu, A., Pereira, H. A., Teodorescu, R., Bongiorno, M., Eremia, M., & Silva, S. R. (2015). Comparison of PI and PR current controllers applied on two-level VSC-HVDC transmission system. *2015 IEEE Eindhoven PowerTech*, 1–5. https://doi.org/10.1109/PTC.2015.7232648

[11] Martinez, J. C. R., Kennel, R. M., & Geyer, T. (2010). Model predictive direct current control. *2010 IEEE International Conference on Industrial Technology*, 1808–1813. https://doi.org/10.1109/ICIT.2010.5472514

[12] Nos, O. V., Makys, P., & Kharitonov, S. A. (2021). Modified resonant controllers with time delay compensation, *2021 XVIII International Scientific Technical Conference Alternating Current Electric Drives (ACED)*, 1–5. https://doi.org/10.1109/ACED50605.2021.9462290

[13] O'Rourke, C. J., Qasim, M. M., Overlin, M. R., & Kirtley, J. L. (2019). A geometric interpretation of reference frames and transformations: Dq0, Clarke, and Park, *IEEE Transactions on Energy Conversion, 34*(4), 2070–2083. https://doi.org/10.1109/TEC.2019.2941175

[14] Tarczewski, T., Skiwski, M., & Grzesiak, L. M. (2017). Constrained non-stationary state feedback speed control of PMSM. *2017 19th European Conference on Power Electronics and Applications (EPE'17 ECCE Europe)*, 1-P.10. https://doi.org/10.23919/EPE17ECCEEurope.2017.8099054

[15] Teodorescu, R., Blaabjerg, F., Liserre, M., & Loh, P. C. (2006). Proportional-resonant controllers and filters for grid-connected voltage-source converters. *IEE Proceedings - Electric Power Applications, 153*(5), 750. https://doi.org/10.1049/ip-epa:20060008

[16] Xie, B., Mao, M., Zhou, L., Wan, Y., & Hao, G. (2020). Systematic design of linear quadratic regulator for digitally controlled grid-connected inverters. *IET Power Electronics, 13*(3), 557–567. https://doi.org/10.1049/iet-pel.2019.0514

[17] Xu, J., Qian, H., Hu, Y., Bian, S., & Xie, S. (2021). Overview of SOGI-Based Single-Phase Phase-Locked Loops for Grid Synchronization Under Complex Grid Conditions. *IEEE Access, 9*, 39275–39291. https://doi.org/10.1109/ACCESS.2021.3063774

[18] Yang, Y., Hadjidemetriou, L., Blaabjerg, F., & Kyriakides, E. (2015). Benchmarking of phase locked loop based synchronization techniques for grid-connected inverter systems. *2015 9th International Conference on Power Electronics and ECCE Asia (ICPE-ECCE Asia)*, 2167–2174. https://doi.org/10.1109/ICPE.2015.7168077

[19] Zammit, D., Staines, C. S., & Apap, M. (2014). Comparison between PI and PR current controllers in grid connected PV inverters. *International Journal of Electrical and Computer Engineering, 8*(2), 6.

[20] Zhang, N., Tang, H., & Yao, C. (2014). A systematic method for designing a PR controller and active damping of the LCL Filter for single-phase grid-connected PV inverters, *Energies, 7*(6), 3934–3954. https://doi.org/10.3390/en7063934

[21] Zmood, D. N., & Holmes, D. G. (2003). Stationary frame current regulation of PWM inverters with zero steady-state error, *IEEE Transactions on Power Electronics*, *18*(3), 814–822. https://doi.org/10.1109/TPEL.2003.810852

[22] Hasanzadeh, A., Edrington, C. S., Maghsoudlou, B., & Mokhtari, H. (2011). Optimal LQR-based multi-loop linear control strategy for UPS inverter applications using resonant controller, *IEEE Conference on Decision and Control and European Control Conference*, 3080–3085. https://doi.org/10.1109/CDC.2011.6161192